Transpl Int (1996) 9: 175–183

ORIGINAL ARTICLE

Nicolau Beckmann
Joanne Joergensen
Konrad Bruttel
Markus Rudin
Henk-Jan Schuurman

Magnetic resonance imaging for the evaluation of rejection of a kidney allograft in the rat

Received: 18 July 1995
Received after revision: 16 November 1995
Accepted: 20 December 1995

N. Beckmann · J. Joergensen · K. Bruttel
M. Rudin · H-J. Schuurman (✉)
Preclinical Research,
Sandoz Pharma Ltd.,
Building 386/101B,
CH-4002 Basel, Switzerland
Fax: + 41 61 324 2379

Abstract Orthotopic DA ($RT1^a$) into Lewis ($RT1^l$) rat kidney allografts and control Lewis-into-Lewis grafts were assessed by magnetic resonance imaging (MRI) and perfusion measurement after intravenous injection of a superparamagnetic contrast agent. MRI anatomical scores (range 1–6) and perfusion rates were compared with graft histology (rank of rejection score 1–6). Not only acute rejection, but also chronic events were monitored after acute rejection was prevented by daily cyclosporine (Sandimmune) treatment during the first 2 weeks after transplantation. In acute allograft rejection ($n = 11$), MRI scores reached the maximum value of 6 and perfusion rates were severely reduced within 5 days after transplantation; histology showed severe acute rejection (histologic score 5–6). In the chronic phase (100–130 days after transplantation), allografts ($n = 5$) manifested rejection (in histology cellular rejection and vessel changes), accompanied by MRI scores of around 2–3 and reduced perfusion rates. Both in the acute and chronic phases, the MRI anatomical score correlated significantly with the histological score (Spearman rank correlation coefficient r_s 0.89, $n = 30$, $P < 0.01$), and perfusion rates correlated significantly with the MRI score or histological score (r_s values between –0.60 and –0.87, $n = 23$, $P < 0.01$). It is concluded that MRI represents an interesting tool for assessing the anatomical and hemodynamical status of a kidney allograft in the acute and chronic phases after transplantation.

Key words MRI, rejection, kidney · Kidney, MRI, rejection · Rejection, MRI, kidney

Introduction

In the preclinical evaluation of immunosuppressive drugs developed for clinical transplantation, organ allografting in rodents is a relevant in vivo experimental approach. One of the models applied is orthotopic kidney allografting in rats using the strain combination of DA ($RT1^a$) into Lewis ($RT1^l$). This strain combination is generally considered to be a very stringent one because of the major histocompatibility mismatch between donor and recipient. In the experimental design, a contralateral nephrectomy is performed at day 7 after transplantation and the graft is inspected. At that time point, untreated animals show macroscopic signs of rejection, such as enlargement of the graft, a reddening of the graft related to hemorrhage, and perigraft inflammation. If left untreated, animals with acute rejection die at around day 11 after transplantation due to the loss of graft function. Long-term survival of the graft is achieved in recipients treated with cyclosporine (Sandimmune) starting from the day of transplantation until day 14 after transplantation. Usually, experiments with long-term survival are terminated between 100 and 130 days after transplantation [2].

In histological assessment, grafts with acute rejection show mononuclear cell infiltration and tubular damage.

A graft with long-term survival resembles a normal kidney with some mononuclear cell infiltration but without damage of the renal parenchyma. Some grafts may show a variable extent of cellular rejection accompanied by vasculopathy, including thickening of vascular walls with proliferation of smooth muscle cells and (neo)intima formation, in severe cases with obstruction of the blood vessel. These features are compatible with chronic rejection and may occur in animals that are apparently healthy and do not show signs of decreased renal function. Such animals may show an increase in serum creatinine; however, in our experience, serum creatinine is not a suitable parameter of graft function due to a lack of sensitivity. Increased creatinine levels, up to 200 μmol/l, may occur after kidney transplantation in animals that show no signs of renal disease when inspected.

When determining graft survival and, hence, the efficacy of the immunosuppressive treatment, animal health associated with graft function (i.e., survival) and histology of the graft at autopsy are the main parameters. In our search for other parameters that are not invasive and that do not require sacrificing the animal, we evaluated nuclear magnetic resonance imaging (MRI). MRI and MR spectroscopy have been applied to study heart and liver transplantation in the rat [3, 5, 7, 8, 10, 14, 18] and kidney grafting in dogs [4]. For kidney allografts in rats, ^{31}P nuclear magnetic resonance has been applied to obtain biochemical data related to parenchymal tissue injury (increase in inorganic phosphate, decrease in β-ATP); for accurate measurements, the graft has had to be implanted in the groin of the recipient animal [13]. This application of nuclear magnetic resonance differs from our approach in which anatomical imaging of orthotopic grafts was the first aim. In addition, we assessed kidney perfusion using a bolus tracking method originally developed to measure local cerebral blood flow [9, 17]. The intravascular paramagnetic or superparamagnetic contrast agent leads to local changes in magnetic susceptibility, which manifests itself as a decrease in the signal intensity in gradient-recalled echo experiments. This signal attenuation in a specific region-of-interest is related to the local tracer concentration and, thus, to the tissue blood volume from which perfusion rates can be derived using the central volume principle. The determination of absolute perfusion rates, however, is not feasible due to fundamental problems in the determination of the mean transit time or the mean residence time of the tracer in the tissue. In fact, it has been shown that the first moment of the signal intensity versus time profile is not equal to the mean transit or residence times [19]. This aside, it is possible to assess relative perfusion rates with a bolus tracking method.

In the experimental design of this study, acute allograft rejection was induced in Lewis rat recipients of a DA kidney and compared with syngeneic Lewis kidney grafts. Chronic rejection was studied in Lewis recipients of a DA kidney that had received a 14-day course of cyclosporine to prevent acute allograft rejection. Also, in this case, the kidney allograft was compared with a syngeneic Lewis kidney graft. To enable an adequate comparison of the graft with a normal kidney, contralateral nephrectomy was not included in the experimental design.

Materials and methods

Animals and experimental design

The study was performed in accordance with the Swiss Animal Welfare Act, dated 9 March 1978, and the accompanying Animal Welfare Regulation dated 28 May 1981. Male DA ($RT1^a$) rats and Lewis ($RT1^l$) rats were obtained from Olac (Bicester, UK) at about 8–10 weeks of age. Two studies were performed. The first study addressed acute rejection and included three groups of animals. Four Lewis rats received a kidney graft from a syngeneic Lewis rat, 11 animals received an allograft with no treatment, and 7 received an allograft and were treated with cyclosporine (Sandimmune) at a dose of 7.5 mg/kg per day p.o. for the duration of the experiment. Animals were analyzed via MRI on days 1, 2, 3, 5, 6, 8, 10, 12, and 14, and autopsy was carried out on days 3, 4, 7, 8, 10, or 14. In the second study, long-term survival was addressed in two groups. Three Lewis rats received a syngeneic kidney graft; five others received a kidney allograft and were treated with cyclosporine (Sandimmune) at a dose of 7.5 mg/kg per day p.o. for 14 days starting from the day of transplantation. MR images were recorded on days 3, 7, 10, and 14 and then at weekly intervals up to day 133 after transplantation. Autopsy was carried out on days 100, 119, 120, 126, or 133. In all animals relative graft perfusion was assessed immediately before sacrifice.

Surgery

Orthotopic kidney transplantation was performed under anesthesia with isoflurane, 1 ml 5 % chloral hydrate i.p., and 0.05 mg atropine sulphate s.c. After removal of the recipient's kidney, the donor kidney was placed in position with end-to-end anastomoses of the renal arteries using 10/0 Ethilon interrupted sutures and of the veins using 10/0 continuous suture. Ureters were anastomosed end-to-end with 10/0 Ethilon interrupted sutures. The ischemia time was about 25 min, 15 min of which was cold; during the other 10 min, the graft was rewarmed. There was no ex vivo perfusion of the graft.

Magnetic resonance imaging

For MRI measurements, animals anesthetized with isoflurane 2 % in a nitrous oxide/oxygen (2:1) mixture administered via a face mask were placed in supine position on a plexiglass support. The respiratory signal, measured with an elastic belt containing a strain gauge fixed around the chest, was recorded with a Physiogard SM 785 monitoring device (Bruker, Karlsruhe, Germany). Conventional MR images were acquired using a Biospec 47/15 spectrometer (Bruker). A homebuilt resonator [1] with a 70-mm inner diameter was used as radiofrequency transmitter/receiver. Spin echo

(SE) pulse sequences with repetition delays of 1000 and 2000 ms and echo delays of 21 and 60 ms [SE(1000/21) and SE(2000/60), respectively] were applied. In order to minimize breathing artifacts, data acquisition was triggered by respiration. The field-of-view was set at 60×60 mm^2, the slice thickness at 1 mm, and ten transverse slices were recorded. The matrix dimension was 256×128, corresponding to pixel dimensions of 0.23×0.47 mm^2. The total measurement time was approximately 4.3 min for SE(1000/21) and 8.5 min for SE(2000/60), with two acquisitions being averaged.

MRI perfusion measurements

Perfusion measurements were carried out on a Biospec 47/40 spectrometer (Bruker) equipped with a self-shielded gradient system. A birdcage resonator [16] with a 70-mm inner diameter was used as a radiofrequency transmitter and receiver. Images were recorded in 1 s using a snapshot sequence [6] with an echo delay of 4.5 ms and a repetition time of 8.3 ms. The field-of-view was 60×60 mm^2, the slice thickness 1 mm, and one coronal slice was measured sequentially 64 times. After the 20th image, a superparamagnetic contrast agent was injected via the tail vein for approximately 1 s. Changes in signal intensity upon injection of the contrast agent were monitored as a function of time. Superparamagnetic magnetite nanoparticles [15] coated with bovine serum albumin were used as a contrast agent. The iron concentration was 5 mg/ml and the volume administered was 0.5 ml.

Histology

At autopsy, the grafted kidney was harvested, fixed in buffered formalin, and embedded in paraffin. Sections 3.5 μm thick were stained with hematoxylin and eosin. Histological changes were scored for the extent of rejection as follows: score 0, normal kidney architecture, no signs of rejection; score 1, slight infiltration of renal parenchyma without signs of rejection; score 2, infiltration with signs of cellular rejection with marginal destruction of renal parenchyma; score 3, cellular rejection with slight destruction of renal parenchyma; score 4, cellular rejection with moderate tissue destruction; score 5, cellular rejection with severe tissue destruction; score 6, end-stage rejection with almost complete destruction of the graft. These scores are illustrated in Fig. 1 for acute rejection and in Fig. 2 for chronic rejection.

Data analysis

Anatomical MR images were analyzed by a person blinded to the treatment. Kidneys were scored as follows: 1, normal; 2, slightly enlarged with some loss of cortical/medullary contrast; 3, severely enlarged; 4, very large with predominantly medullary hemorrhages; 5, very large with focal hemorrhages in the cortex and involvement of adjacent tissue structures; and 6, very large with complete loss of internal structure and severe involvement of the adjacent tissue. Graft perfusion was assessed by measuring the signal profile during passage of an intravascular contrast agent. As the tracer passes the imaging plane, the signal is attenuated; the decrease in signal intensity is related to the amount of tracer in the tissue, thus being a measure for the local exchangeable tissue blood volume [11, 17]. The average signal intensity was determined in regions-of-interest in kidney cortex and medulla for both the transplanted and the contralateral native kidney. The average signal attenuation during the first pass of the contrast agent relative to the precontrast signal intensity was estimated for each region-of-interest. The attenuation values of the transplanted kidney were then expressed as a percent of the values for the contralateral native kidney, i.e., flow(transpl)/flow(contralateral)attenuation(transpl)/attenuation (contralateral), and used as an index for relative perfusion.

Statistical analysis

The nonparametric Spearman rank correlation coefficient (r_s), corrected for ties, was calculated.

Results

MRI scores are illustrated by the images in Fig. 3, which show transverse sections of transplanted kidneys in comparison to the contralateral native kidney. The corresponding score is indicated in the respective image. Compared to SE(1000/21) images, the SE(2000/60) images generally provided a better contrast and allowed differentiation between cortex and medulla at the expense of an increased susceptibility to motion artifacts. A very intense (bright) signal was observed in the pelvis and was due to the presence of urine. Kidneys with acute and chronic rejection showed no obvious differences in gross morphology using the two MRI pulse sequences. Therefore, data are pooled for acute and chronic rejection.

Histology of syngeneic (Lewis-derived) kidney grafts at each time point assessed after transplantation showed a normal kidney architecture. Some infiltration by mononuclear cells (score 1) was observed in grafts at day 8, 10, or 14 after transplantation. This was also found in one of the three long-term survivors. Allogeneic (DA-derived) kidney grafts in animals that received no immunosuppression showed rejection (score 3–4) at day 3 and 4 after transplantation. On day 7 after transplantation and later on, end-stage rejection was observed (score 6). Allografts from three of seven animals treated with cyclosporine during days 3 and 14 after transplantation showed some infiltration without signs of rejection (score 1); three others showed slight rejection (score 2), and in one animal severe rejection (score 5) was observed. In the series of five long-term survivors, two showed marginal rejection (score 2, days 119 and 133 after transplantation), one showed severe rejection (score 5, day 119), and two others showed end-stage rejection (score 6, both at day 100 after transplantation). Rejection in long-term survivors was associated with vessel pathology, but in none of the cases was a complete obstruction of blood vessels evident in the histological section.

The correlation between MRI scores and histological scores is shown in Fig. 4. MRI values corresponded to the measurement on the same day that animals were autopsied. A highly significant correlation between MRI score and rejection score was calculated ($r_s = 0.89$, $P < 0.01$). Changes in MRI score during the time after

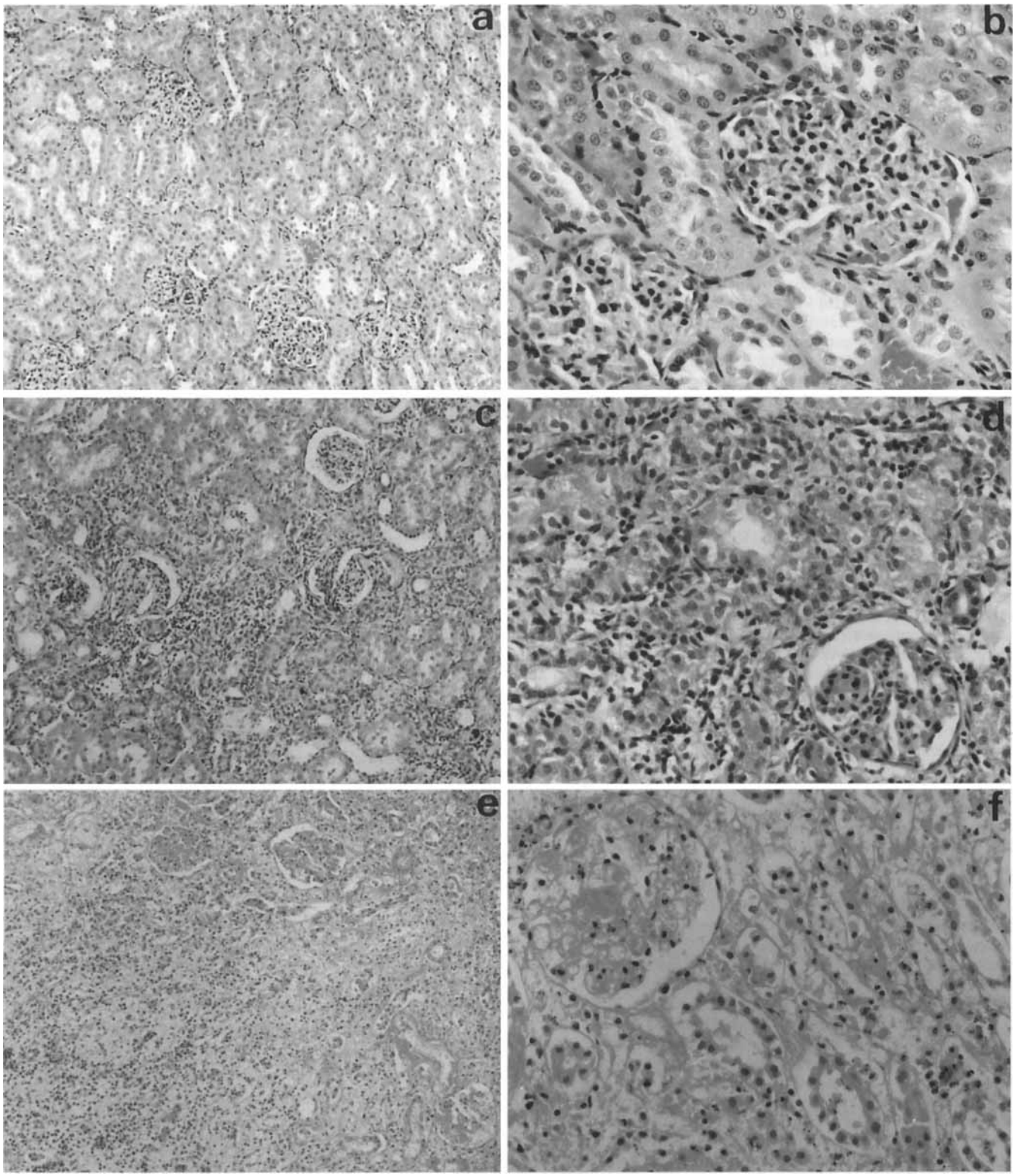

Fig. 1a–f Histology of acute rejection shown at 100x (**a,c,e**) and 250x (**b,d,f**) magnification: **a,b** normal graft, histology score 0; **c,d** slight cellular rejection, histology score 3, with infiltration of the tubular parenchyma and invasion of tubules by lymphocytes (*arrow*); **e,f** end-stage cellular rejection, histology score 6, with almost complete tissue destruction, the structure of a glomerulus relatively maintained

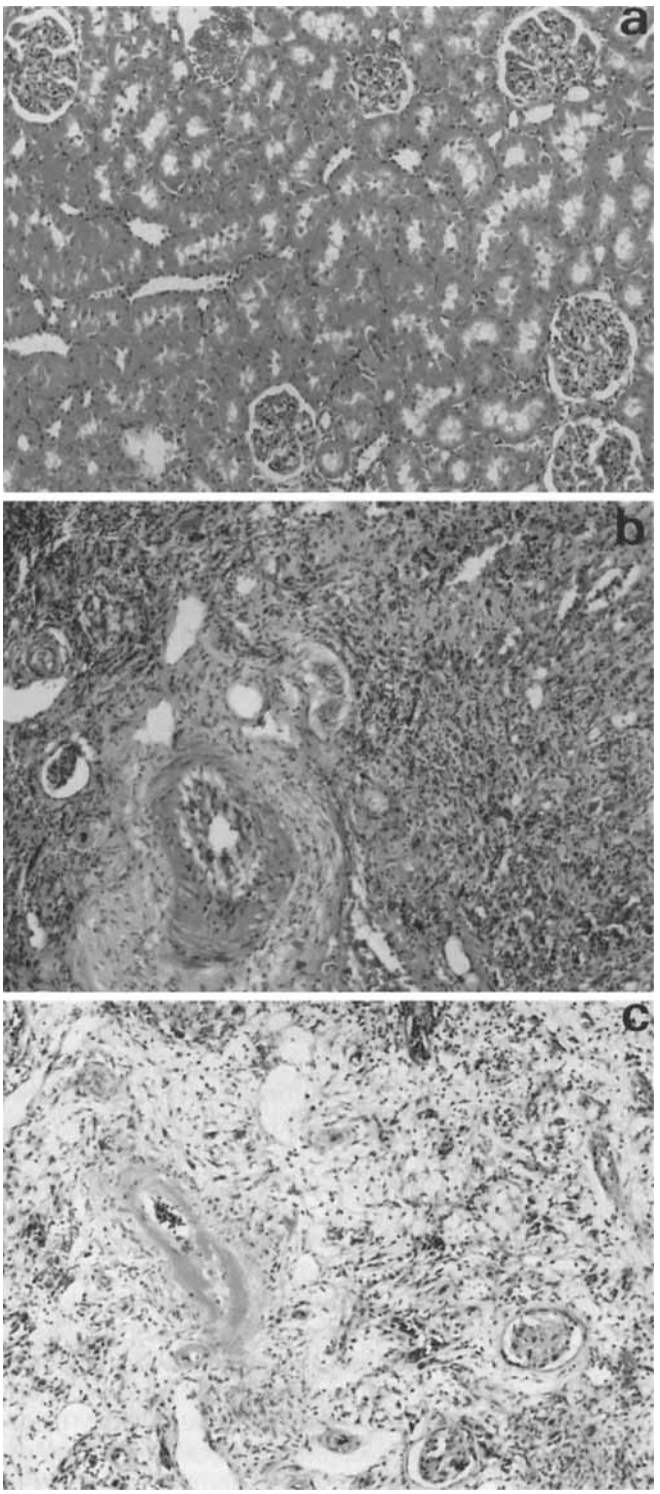

Fig. 2a–c Histology of chronic rejection shown at 100x magnification: **a** allograft after long-term survival without signs of rejection (score 0) showing an essentially normal kidney architecture; **b** severe cellular rejection (score 5); **c** end-stage rejection with almost complete destruction of tissue (score 6). Note the vessel change with thickening of the vessel wall and neointima formation; the lumen is narrowed but not obstructed

transplantation are presented in Fig. 5. The appearance of syngeneic kidney grafts was about normal thoughout the experimental period; the maximum score noted was 3, in two out of ten cases. In contrast, kidney allografts in animals that did not receive cyclosporine reached the maximum score of 6 within 5 days after transplantation. The allografts in cylosporine-treated animals showed only a mild acute response with scores equal to or below 2 in all cases; this was not significantly different from the response in the syngeneic transplants. However, abnormal MRI images indicative of rejection emerged at times longer than 1 month after transplantation. At day 100, three of five animals had a score of 4 or higher. These three animals showed severe rejection at autopsy. The MRI score in two of five long-term surviving allografts that showed marginal rejection at autopsy remained low (score 1) during the experimental period.

Examples of perfusion measurements in the cortex of a syngeneic and of an allogeneic kidney graft are shown in Fig. 6. After entry of the tracer in the tissue, the signal intensity is decreased to about 25 % of its original value within 2–5 s after the injection and then rapidly recovers to about 60 %. This partial recovery reflects recirculation and it takes several minutes before the tracer is cleared from the blood (> 95 % of the original signal intensity). In almost all of the profiles, a second minimum occurred 7–10 s after the injection. The signal profile corresponding to the cortical (Fig. 6 a) and medullary regions-of-interest in syngeneic transplants was not different from that of the respective regions-of-interest in the contralateral native kidney of the animal. Kidney allografts during rejection showed a different picture (Fig. 6 b). The tracer uptake was severely compromised in these cases. The signal minimum after 2–5 s, reflecting the first pass of the tracer, was not observed. Only at 20–25 s after tracer infusion were tracer plasma equilibrium levels reached in the region-of-interest. This profile is indicative of severely affected kidney perfusion. There were no significant differences in perfusion rates between grafts with an acute or chronic rejection. Therefore the data of perfusion measurements during the acute and chronic phases after transplantation have been combined.

The correlation of the perfusion rate and the scores obtained with MRI and graft histology are shown in Fig. 7. In all combinations, the correlation between perfusion rate of cortex or medulla and score by MRI or histology was statistically significant (r_s values between –0.60 and –0.87, $P < 0.01$). For MRI scores 1 and 2, the perfusion rate in the transplanted kidney was essentially normal, but the blood flow was severely compromised in cases of MRI scores of 4–6. Of all rats measured, only one had an MRI score of 3 at the time point of perfusion measurement and a perfusion rate of 53 %. Looking at the histological scores, slight (score 3) to moderate (score 4) rejection proved to be associated with a reduced kidney blood flow measured by perfusion.

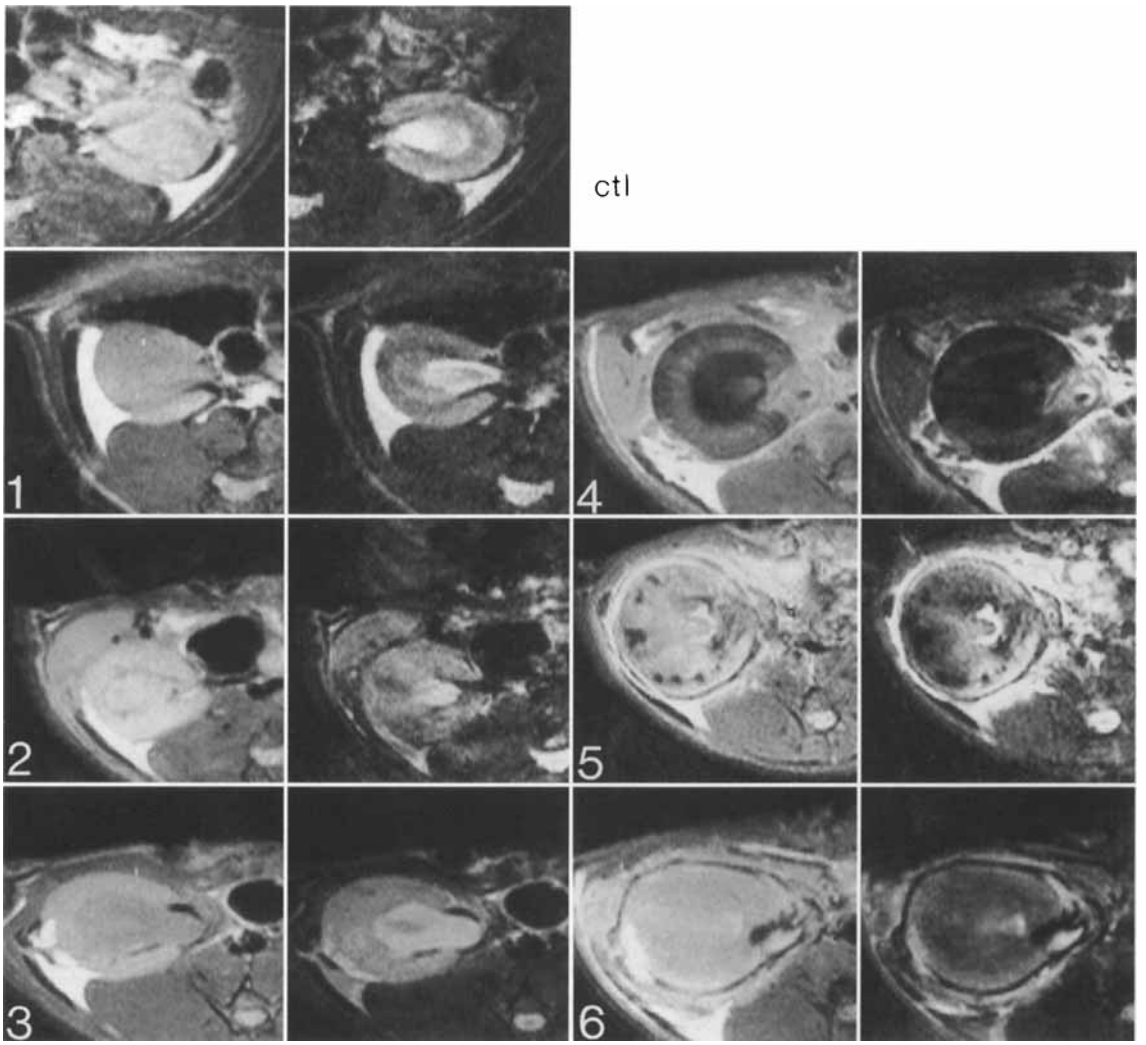

Fig. 3 Transverse sections of the rat kidney, extracted from multislice (ten slices) MRI data sets. The images on the top correspond to the contralateral native kidney. The other images are transverse sections of transplanted kidneys and are presented in opposite orientation. MRI scores indicated in the figure are as follows: *1*, normal; *2*, slightly enlarged kidney with some loss of contrast between cortex and medulla; *3*, severely enlarged kidney; *4*, very large kidney with predominantly medullary hemorrhages; *5*, very large kidney with focal hemorrhages in the cortex and involvement of adjacent tissue structures; *6*, very large kidney with loss of cortical and medullary structure and severe involvement of the adjacent tissue. For each illustration, the image on the *left* side corresponds to an SE(1000/21) acquisition, and that on the *right* side corresponds to an SE(2000/60) acquisition. The data acquisition was triggered by respiration

Discussion

Respiratory-gated MRI yields images of good quality from the rat kidney, enabling one to differentiate between cortex and medulla areas. The SE(1000/21) images essentially revealed proton density maps, allowing us to assess the overall kidney dimensions. The SE(2000/60) images provided a better tissue contrast, and structures like cortex, medulla, and pelvis (urine) could be identified (Fig. 3). Due to the longer echo time (60 ms), however, the latter sequence was more prone to artifacts (respiration, pulsatile blood flow, intestinal motility). Therefore, both sequences were used in the present study. In syngeneic kidney grafts, MRI did not reveal any morphological changes. This was confirmed by normal kidney histology at autopsy. There was only one exception, in which T_2-weighted MR images attained using the SE(2000/60) pulse sequence revealed a very large kidney pelvis, indicative of an obstructed ureter. The kidney tissue itself seemed unaffected, i.e., neither hemorrhage nor loss of cortical/medullar contrast was observed.

Kidney allografts in rats receiving no treatment manifested severe rejection within 7 days, and this was confirmed by histology (Fig. 2). In these cases, MR imaging

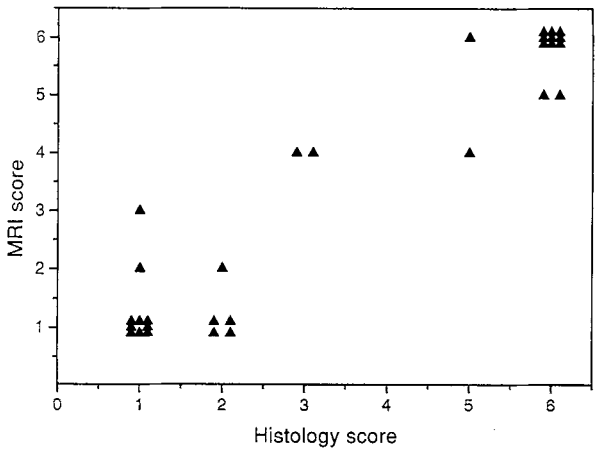

Fig. 4 Correlation between MRI score and histologic score of rejection. The nonparametric Spearman rank correlation coefficient (r_s), corrected for ties, was 0.89 ($n = 30$, $P < 0.01$)

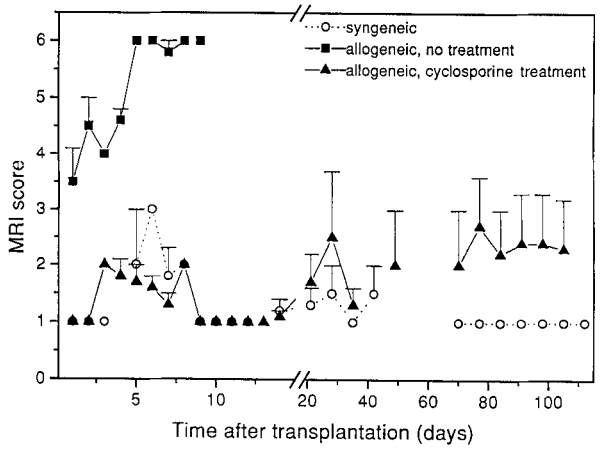

Fig. 5 Changes in MRI scores of kidney grafts in time after transplantation presented for syngeneic transplantation and allogeneic transplantation with or without cyclosporine treatment. Data presented represent mean values ± SEM

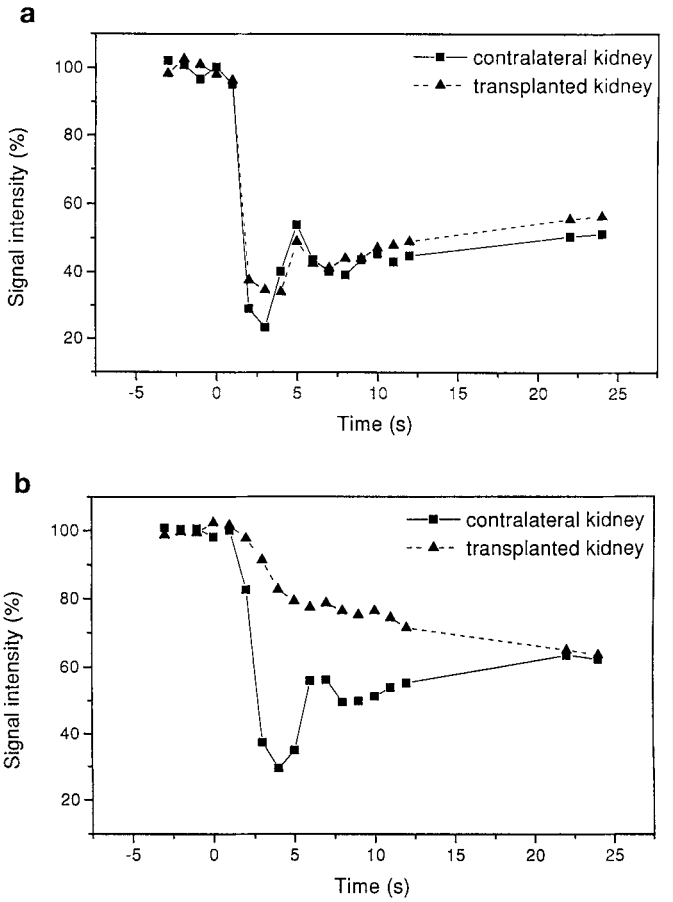

Fig. 6 a,b Relative intensity of the MR signal averaged over a region-of-interest in the kidney cortex for snapshot images acquired sequentially (acquisition time of one image was 1 s). At timepoint 0, 0.5 ml of the contrast agent ($(Fe_3O_4)_x$BSA, 5 mg/ml) was injected into the tail vein for 1 s. In each figure, the relative intensities of the transplanted kidney and the contralateral native kidney of the animal are presented: **a** syngeneic kidney graft without rejection, 90 days after transplantation, showing a similar profile in time for the transplanted and native kidney; **b** kidney allograft with cellular rejection, 75 days after transplantation, showing a severely reduced attenuation of the signal intensity in the graft

revealed a striking feature of the involvement of the adjacent structures. The zone of hyperintense signals surrounding the kidney was due to increased T_2 values associated with increased local tissue water (edema). This is indicative of an inflammatory process that is part of the rejection process.

According to our expectations, there was no, or only slight, cellular rejection in allografted recipients that received cyclosporine immunosuppression. The MRI score in these animals was low (≤ 2) during the initial period after transplantation (Fig. 5), and graft perfusion rate was as in the contralateral native kidney. Only in one case was a very large hemorrhagic kidney observed in MR images and severe rejection (score 5) in histology. This occurrence of rejection is related to the dose of cyclosporine administered; in our experience with this stringent Lewis/DA rat strain combination, a daily dose of 7.5 mg/kg per day given p.o. during the first 2 weeks after transplantation generally results in long-term survival, but some cases may show acute cellular rejection. This also underlies the emergence of chronic rejection at a later phase. Apparently, the dose of cyclosporine administered is just sufficient to prevent acute rejection in most cases, but not sufficient to induce tolerance in the animals in such a way that chronic rejection is also prevented. Three of five animals with long-term survival showed severe to end-stage rejection at autopsy and MRI scores of 4 to 5. In these cases, there were no clear signs of the presence of hemorrhages on

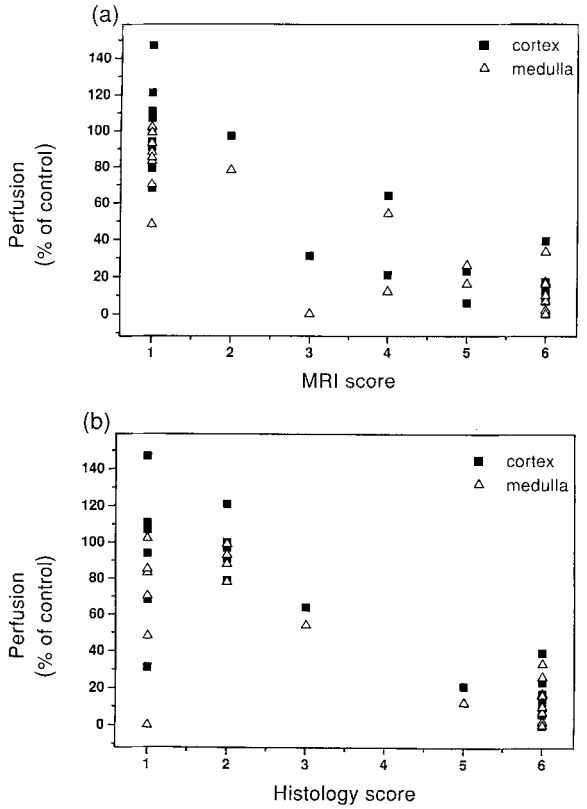

Fig. 7a,b Correlation between graft perfusion rate in the cortex (■; △) and the medulla and **a** MRI scores and **b** histological scores. The Spearman rank correlation coefficients (r_s) were: perfusion cortex vs MRI score –0.87 ($n = 23$, $P < 0.01$); perfusion medulla vs MRI score –0.80 ($n = 23$, $P < 0.01$); perfusion cortex vs histology score –0.82 ($n = 23$, $P < 0.01$); perfusion medulla vs histology score –0.60 ($n = 23$, $P < 0.01$)

MRI anatomical images, which contrasts to pictures in cases with acute rejection. However, all of the animals with chronic rejection had a significantly enlarged kidney pelvis, indicative of an imbalance between urine production and clearance. This difference from grafts showing acute rejection may be ascribed to the chronicity of the rejection process which, in addition to attacking the tubular parenchyma, involves glomeruli and vessel pathology. According to histology, the cellular type of rejection was invariably present, enabling us to apply the same scoring system to describe rejection in the acute phase and in long-term surviving grafts. Histological scoring, however, provides no information on altered perfusion due to vessel damage and graft size; both parameters can be assessed by MRI and the values recorded correlated with histological data.

The signal profiles from perfusion assessment shown in Fig. 6 indicate that the temporal resolution has to be of the order of 1 s or better to follow the first pass of the tracer bolus. The time dependence of the signal intensity in rejected kidneys is indicative of severely compromised graft perfusion, comparable to profiles observed in cerebral ischemia [12]. The relative perfusion rates, obtained from the comparison of grafted and contralateral native kidneys, significantly correlated with the scores by MR imaging and histology (Fig. 7). A significant lowering of perfusion already occurred with slight rejection (scores 3).

The present data on MRI parameters and histology were obtained in the experimental condition that the graft had no life-supporting function, i.e., the contralateral native kidney was kept in place. This design was chosen to enable a comparison between the animal's own native kidney, not under attack by the potential immune response, and the grafted kidney allograft. This implies that possible systemic, metabolic disturbances related to impaired renal function due to rejection and/or adverse drug side effects (e.g., hypertension) presumably did not occur in the animals and, hence, could not interfere with the graft status. We have extended the present studies to include an assessment of animals subjected to contralateral nephrectomy after kidney allografting with essentially similar results (data not shown).

In conclusion, we show that in vivo MRI represents an interesting tool for assessing the status of a kidney allograft, both in the acute and chronic phases after transplantation. The method provides relevant information on both anatomical and hemodynamic aspects, both of which correlated significantly with graft histology. This raises the possibility of assessing the status of the graft at multiple time points during an experimental period. This phenomenon has relevance for the preclinical evaluation of drugs for their efficacy in treating ongoing rejection reactions and in monitoring the graft more closely during treatment regimens. Thus, MRI serves as a valuable addition to the present armamentarium with which one can assess the rat kidney allograft status, even though the direct pathological-anatomical examination is still the "gold standard". MR imaging is also of value in the assessment of graft function using contrast agents that are predominantly cleared in the kidney, such as gadolinium-diethylenetriamine-pentaacetate.

References

1. Alderman DW, Grant DM (1979) An efficient decoupler coil design which reduces heating on conductive samples in superconducting spectrometers. J Magn Reson Imaging 36: 447–454
2. Borel JF (1989) Pharmacology of cyclosporine (Sandimmune). IV. Pharmacological properties in vivo. Pharmacol Rev 41: 259–371
3. Bowers JL, Teramoto K, Khettry U, Clouse ME (1992) ^{31}P NMR assessment of orthotopic rat liver transplant viability. The effect of warm ischemia. Transplantation 54: 604–609
4. Bretan PN, Vigneron DB, Hricak H, Price DC, Yen TS, Luo JA, Tangho EA, James TL (1993) Assessment of in situ renal transplant viability by ^{31}P-MRS: experimental study in canines. Am Surg 59: 182–187
5. Fraser CD, Chacko VP, Jacobus WE, Mueller P, Soulen RL, Hutchins GM, Reitz BA Baumgartner WA (1990) Early phosphorus 31 nuclear magnetic resonance bioenergetic changes potentially predict rejection in heterotopic cardiac allografts. J Heart Transplant 9: 197–204
6. Haase A (1990) Snapshot FLASH MRI. Applications to T_1, T_2, and chemical shift imaging. Magn Reson Med 13: 77–89
7. Konstam MA, Aronovitz MJ, Runge VM, Isner JM, Foster EA, Kaufman DM, Diehl JT, Dresdale AR, Katzen NA, Kaplan E (1991) Magnetic resonance imaging in ischemic injury after heart transplantation in rats. J Heart Lung Transplant 10: 750–756
8. Mühler A, Freise CE, Kuwatsuru R, Rosenau W, Liu T, Mintorovitch J, Clement O, Vexler V, Mahboubi S, Lang P, Roberts JP, Brasch RC (1993) Acute liver rejection: evaluation with cell-directed MR contrast agents in a rat transplantation model. Radiology 186: 139–146
9. Rosen BR, Belliveau JW, Vevea JM, Brady TJ (1990) Perfusion imaging with NMR contrast agents. Magn Reson Med 14: 249–265
10. Rozenman Y, Kantor HL (1990) Heterotopic transplanted rat heart: a model for in vivo determination of phosphorus metabolites during ischemia and reperfusion. Magn Reson Med 13: 450–457
11. Rudin M, Sauter A (1991) Noninvasive determination of regional cerebral blood flow in rats using dynamic imaging with Gd(DTPA). Magn Reson Med 22: 32–46
12. Rudin M, Beckmann N, Sauter A, Tiefenauer L (1994) Assessment of brain perfusion in the rat using snapshot NMR and an intravascular contrast agent. In: Society of Magnetic Resonance, 2nd meeting, San Francisco, August 1994. Book of abstracts, p 1026
13. Shapiro JI, Haug CE, Shanley PF, Weil III R, Chan L (1988) ^{31}P nuclear magnetic resonance study of renal allograft rejection in the rat. Transplantation 45: 17–21
14. Suzuki S, Kanashiro M, Hayashi R, Kenmochi T, Fukuoka T, Amemiya H (1990) In vivo ^{31}P nuclear magnetic resonance findings on heterotopically allografted hearts in rats treated with a novel immunosuppressant, FK 506. Heart Vessels 5: 224–229
15. Tiefenauer LX, Kühne G, Andres RY (1993) Antibody-magnetite nanoparticles: in vitro characterization of a potential tumor specific contrast agent for magnetic resonance imaging. Bioconjug Chem 4: 347–352
16. Tropp J (1989) The theory of the birdcage resonator. J Magn Reson Imaging 82: 51–52
17. Villringer A, Rosen BR, Belliveau JW, Ackerman JL, Lauffer RB, Buxton RD, Chao YS, Wedeen VJ, Brady TJ (1988) Dynamic imaging with lanthanide chelates in normal brain: contrast due to magnetic susceptibility effects. Magn Reson Med 6: 164–174
18. Walpoth BH, Tschopp A, Lazeyras F, Galdikas J, Tschudi J, Altermatt H, Schaffner T, Aue WP, Althaus U (1993) Magnetic resonance spectroscopy for assessing myocardial rejection in the transplanted rat heart. J Heart Lung Transplant 12: 271–282
19. Weisskoff RM, Chesler D, Boxerman JL, Rosen BR (1993) Pitfalls in MR measurements of tissue blood flow with intravascular tracers: which mean transit time? Magn Reson Med 29: 553–558